URSI GASS 2020, Rome, Italy, 29 August - 5 September 2020

Eigenfrequency Spectrum of Prolate Spheroidal Magneto-optic Cavities

Grigorios P. Zouros[(1)], Georgios D. Kolezas[(1)], Gerasimos K. Pagiatakis[(2)], and John A. Roumeliotis[(1)]
(1) School of Electrical and Computer Engineering, National Technical University of Athens, 15780 Athens, Greece
(2) Department of Electrical and Electronic Engineering Educators, School of Pedagogical and Technological Education, 14121 Athens, Greece

Abstract

In this work we report on the eigenfrequencies of magneto-optic cavities, their non-degeneration, and their sensitivity, when the cavity deviates from the traditional spherical shape and deforms, due to manufacturing defects, into a prolate spheroid. Since the cavity is statically magnetized due to an external magnetic bias, its permittivity tensor becomes gyroelectric. To solve this problem, we employ a technique based on spheroidal eigenvectors for the expansion of the electromagnetic field in the anisotropic region of the cavity. The eigenfrequencies are obtained by setting system's matrix determinant equal to zero, with the matrix being obtained after the satisfaction of the boundary conditions at the spheroidal surface. Comparisons with a shape-perturbation technique are performed, and numerical results on the eigenfrequency spectrum are given for different aspect ratio magneto-optic cavities.

1 Introduction

Recently, there has been significant activity in studying the magneto-optical coupling between spin and electromagnetic waves in the visible or near-infrared part of the spectrum [1]–[5]. Such a coupling can be realized in the so-called optomagnonic cavities which are mainly spherical resonators composed of bismuth-substituted yttrium iron garnets (Bi:YIG). In the near-infrared spectrum, this magnetic garnet presents a gyroelectric permittivity tensor of the form $\overline{\overline{\varepsilon}} = \varepsilon\varepsilon_0(\hat{x}\hat{x}+\hat{y}\hat{y}+\hat{z}\hat{z}) - ig\varepsilon_0(\hat{x}\hat{y}-\hat{y}\hat{x})$, where ε is the relative permittivity, g is Faraday coefficient [6], and ε_0 is free space permittivity. The value of the off-diagonal element g depends on bismuth substitution and is generally small [7]. The permeability of the cavity equals free space permeability μ_0.

The typical configuration for implementing magneto-optical coupling is through spherical cavities. In this work, we take a step further and extract the eigenfrequencies of prolate spheroidal magneto-optic cavities, which may be considered as squeezed spheres, due to manufacturing defects. The spheroidal cavity has a major axis of length $2c_0$, a minor axis of length $2b_0$, an interfocal distance $d = 2a$, and an aspect ratio $c_0/b_0 = (1-h^2)^{-1/2}$, where $h = a/c_0$ is the eccentricity. Its permittivity is $\overline{\overline{\varepsilon}} = \varepsilon\varepsilon_0(\hat{x}\hat{x}+\hat{y}\hat{y}+\hat{z}\hat{z}) - ig\varepsilon_0(\hat{x}\hat{y}-\hat{y}\hat{x})$ as described above, while its permeability is μ_0. The background medium of the configuration is free space. To retrieve the eigenfrequencies, we expand the electromagnetic field inside the gyroelectric region in terms of spheroidal eigenvectors featuring a set of discrete wavenumbers that account for the gyroelectric anisotropy, while the incident and scattered electromagnetic field are expanded in terms of spheroidal eigenvectors, featuring the free space wavenumber. Satisfying the boundary conditions at the spheroidal surface, and upon null external excitation, we finally obtain an homogeneous system from which the eigenfrequencies are computed by setting its matrix determinant equal to zero.

2 Solution of the Problem

To expand the electromagnetic field in the gyroelectric region, we first use the following expansion for the electric field in terms of spherical eigenvectors, i.e.,

$$\begin{aligned}\mathbf{E}(\mathbf{r}) = \sum_{m=-\infty}^{\infty}\sum_{n=|m|}^{\infty}\overline{E}_{mn}\sum_{l=1}^{\infty}a_l\Big[&c_{mnl}\mathbf{M}_{mn}^{(1)}(k_l,\mathbf{r}) \\ &+ d_{mnl}\mathbf{N}_{mn}^{(1)}(k_l,\mathbf{r}) + \frac{\overline{w}_{mnl}}{\lambda_l}\mathbf{L}_{mn}^{(1)}(k_l,\mathbf{r})\Big] \\ &+ \sum_{l=1}^{\infty}a_l\frac{w_{00l}}{\lambda_l}\mathbf{L}_{00}^{(1)}(k_l,\mathbf{r}). \qquad (1)\end{aligned}$$

In (1), $\overline{E}_{mn} = i^n[(2n+1)(n-m)!/n/(n+1)/(n+m)!]^{1/2}$, c_{mnl}, d_{mnl}, λ_l, $\overline{w}_{mnl}$ and w_{00l} are obtained by solving an eigenvalue problem, the matrix of which depends on the elements ε and g of the gyroelectric tensor $\overline{\overline{\varepsilon}}$ [8], k_l are discrete wavenumbers given by $k_l = \sqrt{\varepsilon/\lambda_l}k_0$, with k_0 the free space wavenumber, and a_l are unknown expansion coefficients. The divergenceless $\mathbf{M}_{mn}^{(1)}$ and $\mathbf{N}_{mn}^{(1)}$ and the curl-free $\mathbf{L}_{mn}^{(1)}$ vectors appearing in (1) are the well-known spherical eigenvectors [9], while the superscript (1) denotes that the spherical Bessel functions are used in the respective expressions of these vectors. The $\exp(-i\omega t)$ time dependence has been adopted ad suppressed throughout. The expansion of the electric field in the gyroelectric region is completed by transforming $\mathbf{M}_{mn}^{(1)}$, $\mathbf{N}_{mn}^{(1)}$, $\mathbf{L}_{mn}^{(1)}$ into the equivalent spheroidal eigenvectors, by employing appropriate relations [10].

Next, the scattered field is expanded in spheroidal eigen-

vectors as

$$\mathbf{E}^{\mathrm{sc}}(\mathbf{r_s}) = \sum_{m=-\infty}^{\infty} \sum_{n=|m|}^{\infty} \left[A_{mn} \mathbf{M}_{mn}^{r(3)}(c, \mathbf{r_s}) + B_{mn} \mathbf{N}_{mn}^{r(3)}(c, \mathbf{r_s}) \right], \tag{2}$$

where $\mathbf{M}_{mn}^{r(3)}$, $\mathbf{N}_{mn}^{r(3)}$ are the spheroidal eigenvectors of the third kind, $c = k_0 a$, $\mathbf{r_s}$ is the position vector in spheroidal coordinates, and A_{mn}, B_{mn} are unknown expansion coefficients. A similar expansion as in (2) is applied for the incident field [11].

The respective magnetic fields, inside and outside the cavity, are obtained from Faraday's law $\mathbf{H}(\mathbf{r_s}) = -i/(\omega\mu_0)\nabla \times \mathbf{E}(\mathbf{r_s})$. Satisfying the boundary conditions for the continuity of the tangential components of the total electric and magnetic fields at the spheroid's surface, and setting null excitation to form the resonance problem (i.e., setting the incident field equal to zero), we end up with the linear homogeneous system $\mathbb{A}(x_0)\mathbf{v} = 0$, where matrix $\mathbb{A}$ depends on the normalized eigenfrequency (or normalized wavenumber) $x_0 = k_0 c_0$. In principle, the solutions x_0 of the determinantal equation $|\mathbb{A}(x_0)| = 0$ are complex, thus giving rise to complex eigenfrequencies $f = x_0/(2\pi c_0\sqrt{\mu_0\varepsilon_0})$. The real part of f's yields the natural resonance frequencies of the magneto-optic cavity.

3 Numerical Results

In [5] it was shown that a magnetized spherical cavity, formed by Bi:YIG, with typical values $\varepsilon = 5.5$ and $|g| = 0.01$, may be operated at specific eigenmodes at which optomagnonic coupling can be realized. While unmagnetized ($g = 0$), the mode of interest examined in [5] is the TE_{11}, where the value of subscript corresponds to index n. This mode is degenerate (meaning that the eigenfrequencies obtained for any value of m are the same), and has been reported to have $\lambda_0/c_0 = 0.9909$ or $x_0 = 6.34067$, with λ_0 the free space wavelength and c_0 the radius of the sphere [5]. For a typical value of 1-micron radii, the coupling takes place in the near-infrared at 990.934 nm with respective eigenfrequency 302.53 THz. When the sphere is magnetized ($g \neq 0$), the TE mode ceases to exist, and becomes hybrid. Furthermore, the eigenfrequencies become non-degenerate (meaning that for a different value of m, a different eigenfrequency is obtained), and a rich spectrum is revealed. This was illustrated in [5] for $m = \pm 1$ modes, yet, $2n+1$ non-degenerate modes in total exist, where, in the present case, $n = 11$.

We use the method of spheroidal eigenvectors to reveal the non-degenerate eigenfrequencies, which stem from this TE_{11} mode, when the spherical particle becomes magnetized with $\varepsilon = 5.5$ and $g = 0.02$ (in this study we adopt $g = 0.02$ rather than the 0.01 value used in [5] to enhance the gyroelectric effect and illustrate more clearly the various differences appearing due to nonzero g). To do so, we examine the above described determinantal equation $|\mathbb{A}(x_0)| = 0$ by setting $h = 0$ (so the spheroid becomes a sphere), and seek the solutions x_0 by applying a complex root-finding algorithm [13]. We confine our study only in $m = -2, -1, 0, 1, 2$, and not in the full $m = -11, \ldots, 11$ range. The complex x_0 obtained by this method are given in Table 1/first subtable, within a precision of six significant figures. It should be noted that the imaginary part is quite small, revealing that high-Q modes are coupled within the cavity. To validate the results, we apply the following procedure. In Fig. 1, we plot the total scattering cross section Q_t/λ_0^2 for the aforementioned magnetized spherical particle. This is achieved by extending our recent work in [12] to support gyroelectric permittivities. To obtain the scattering spectra, the cavity is illuminated by a TE polarized plane wave, one time with an angle of incidence $\theta_0 = 0^\circ$—where θ_0 is defined as the angle between the incident wavevector and the positive Oz semi-axis—and one time with $\theta_0 = 90^\circ$. The value $\theta_0 = 0^\circ$ reveals only the $m = \pm 1$ modes, since only these two indices are present in the expansion of the incident field in this case [9]. The various modes in the scattering spectra are depicted by the arrows in Fig. 1. The precise values of x_0 are given in Table 1/first subtable. Although the values of x_0 are complex, from Fig. 1 we have collected the real parts (denoted as Re in Table 1). The agreement between the method of spheroidal eigenvectors

Table 1. Normalized eigenfrequencies x_0 for magneto-optic spherical and prolate spheroidal cavities. Values of parameters: $\varepsilon = 5.5$ and $g = 0.02$.

Sphere		
$h = 0$	x_0—this work	$\mathrm{Re}\{x_0\}$—[12]
$m = 2$	$6.34087 - 6.96427 \times 10^{-5} i$	6.34087
$m = 1$	$6.34097 - 6.96901 \times 10^{-5} i$	6.34097
$m = 0$	$6.34105 - 6.97215 \times 10^{-5} i$	6.34106
$m = -1$	$6.34114 - 6.97310 \times 10^{-5} i$	6.34113
$m = -2$	$6.34121 - 6.97150 \times 10^{-5} i$	6.34121
Spheroid		
$h = 0.01$	x_0—this work	$\mathrm{Re}\{x_0\}$—[12]
$m = 2$	$6.34104 - 6.96459 \times 10^{-5} i$	6.34103
$m = 1$	$6.34113 - 6.96928 \times 10^{-5} i$	6.34112
$m = 0$	$6.34121 - 6.97247 \times 10^{-5} i$	6.34119
$m = -1$	$6.34130 - 6.97304 \times 10^{-5} i$	6.34127
$m = -2$	$6.34137 - 6.97147 \times 10^{-5} i$	6.34139
Spheroid		
$h = 0.1$	x_0—this work	
$m = 2$	$6.35755 - 7.05128 \times 10^{-5} i$	
$m = 1$	$6.35726 - 7.04829 \times 10^{-5} i$	
$m = 0$	$6.35719 - 7.04199 \times 10^{-5} i$	
$m = -1$	$6.35736 - 7.03187 \times 10^{-5} i$	
$m = -2$	$6.35776 - 7.01947 \times 10^{-5} i$	
Spheroid		
$h = 0.2$	x_0—this work	
$m = 2$	$6.41003 - 8.00140 \times 10^{-5} i$	
$m = 1$	$6.40851 - 8.00846 \times 10^{-5} i$	
$m = 0$	$6.40796 - 7.98339 \times 10^{-5} i$	
$m = -1$	$6.40840 - 7.92740 \times 10^{-5} i$	
$m = -2$	$6.40981 - 7.84405 \times 10^{-5} i$	

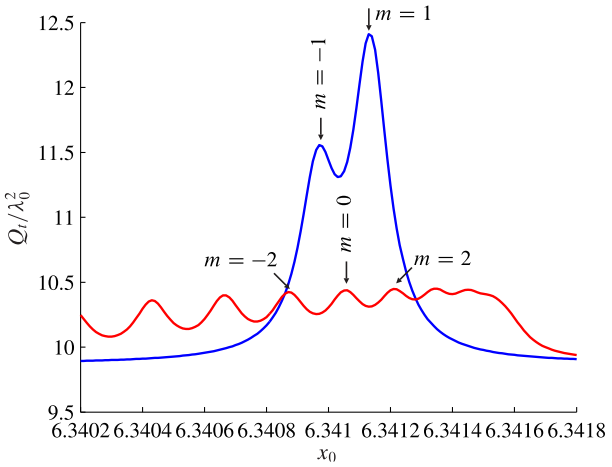

Figure 1. Normalized total scattering cross section Q_t/λ_0^2 versus x_0 for a magnetized sphere with $\varepsilon = 5.5$ and $g = 0.02$, illuminated by a TE polarized plane wave [12]. Blue: $\theta_0 = 0^\circ$; red: $\theta_0 = 90^\circ$.

and [12] is excellent, up to six significant digits.

Setting as a starting point the normalized eigenfrequencies obtained for the gyroelectric sphere with $h = 0$, we introduce a small value in the eccentricity, i.e., $h = 0.01$, and compute the new spectrum for the gyroelectric prolate spheroid using the method of spheroidal eigenvectors. The results are shown in Table 1/second subtable. The eigenfrequencies have now been perturbed. The results obtained from this method are again validated with [12], by following the same procedure as in Fig. 1. Table 1/second subtable reveals that the agreement is up to five significant figures. Next, we proceed by assigning h higher values. As it is evident from Table 1/third subtable, the normalized eigenfrequencies increase in value, as h increases from 0.01 to 0.1. Although this increment in x_0 takes place in the second decimal digit, the increment is much higher when h further increases from 0.1 to 0.2, as it is shown in Table 1/fourth subtable. This behavior reveals the difficulty in obtaining, with a certain degree of accuracy, the complex roots for the magneto-optic spheroidal cavity. Although the change from $h = 0.1$ to $h = 0.2$ is not large, the corresponding values of x_0 differ in the first decimal place, therefore rendering the root-finding procedure a hard task to retrieve the correct root for $h = 0.2$ by simply changing the value from $h = 0.1$ to $h = 0.2$. Consequently, one should proceed by increasing h in small steps, and each new root is obtained, to be used as a starting point in the next step. Obviously, to compute the eigenfrequencies for larger h is a cumbersome and time consuming task. As a final remark we note that, in contrast to the spherical gyroelectric cavity where the real part of x_0 constantly decreases as we move from $m = -2$ to $m = 2$, the $\mathrm{Re}(x_0)$ for the spheroidal gyroelectric cavity does not follow a monotonic property, but rather yields a minimum at $m = 0$. This trend is observed for both the $h = 0.1$ and $h = 0.2$ cases.

4 Conclusions

We have calculated the eigenfrequencies of prolate spheroidal magneto-optic cavities using a method based on spheroidal eigenvectors. Although non-degeneracy is anticipated in gyroelectric cavities, we have shown that eccentricity, not only shifts the eigenfrequencies to higher values, but also that this shift is large even for small changes in eccentricity. This property renders the complex root-finding procedure a difficult task, if one wishes to compute an accurate spectrum.

5 Acknowledgements

This work has been financed by the Greek School of Pedagogical and Technological Education (ASPETE) through the operational program "Research strengthening in ASPETE"—Project "Optomagnonic Devices & Systems (OPTOMAGNON)".

References

[1] J. A. Haigh, S. Langenfeld, N. J. Lambert, J. J. Baumberg, A. J. Ramsay, A. Nunnenkamp, and A. J. Ferguson, "Magneto-optical coupling in whispering-gallery-mode resonators," *Phys. Rev. A*, vol. 92, p. 063845, 2015.

[2] S. V. Kusminskiy, H. X. Tang, and F. Marquardt, "Coupled spin-light dynamics in cavity optomagnonics," *Phys. Rev. A*, vol. 94, p. 033821, 2016.

[3] A. Osada, R. Hisatomi, A. Noguchi, Y. Tabuchi, R. Yamazaki, K. Usami, M. Sadgrove, R. Yalla, M. Nomura, and Y. Nakamura, "Cavity optomagnonics with spin-orbit coupled photons," *Phys. Rev. Lett.*, vol. 116, p. 223601, 2016.

[4] P. A. Pantazopoulos, N. Stefanou, E. Almpanis, and N. Papanikolaou, "Photomagnonic nanocavities for strong light-spin-wave interaction," *Phys. Rev. B*, vol. 96, p. 104425, 2017.

[5] E. Almpanis, "Dielectric magnetic microparticles as photomagnonic cavities: Enhancing the modulation of near-infrared light by spin waves," *Phys. Rev. B*, vol. 97, p. 184406, 2018.

[6] D. D. Stancil and A. Prabhakar, *Spin Waves—Theory and Applications*. New York: Springer Science+Business Media, LLC, 2009.

[7] S. M. Drezdzon and T. Yoshie, "On-chip waveguide isolator based on bismuth iron garnet operating via nonreciprocal single-mode cutoff," *Opt. Expr.*, vol. 17, pp. 9276–9281, 2009.

[8] G. P. Zouros, "Eigenfrequencies and modal analysis of uniaxial, biaxial, and gyroelectric spherical cavities," *IEEE Trans. Microw. Theory Techn.*, vol. 65, pp. 20–27, 2017.

[9] J. A. Stratton, *Electromagnetic Theory*. New York: McGraw-Hill, 1941.

[10] M. F. R. Cooray and I. R. Ciric, "Rotational-translational addition theorems for vector spheroidal wave functions," *COMPEL*, vol. 8, pp. 151–166, 1989.

[11] G. P. Zouros, A. D. Kotsis, and J. A. Roumeliotis, "Efficient calculation of the electromagnetic scattering by lossless or lossy, prolate or oblate dielectric spheroids," *IEEE Trans. Microw. Theory Techn.*, vol. 63, pp. 864–876, 2015.

[12] G. D. Kolezas, G. P. Zouros, and K. L. Tsakmakidis, "Engineering subwavelength nanoantennas in the visible by employing resonant anisotropic nanospheroids," *IEEE J. Sel. Top. Quantum Electron.*, vol. 25, p. 4700912, May/June 2019.

[13] G. P. Zouros, "CCOMP: An efficient algorithm for complex roots computation of determinantal equations," *Comput. Phys. Comm.*, vol. 222, pp. 339–350, 2018.